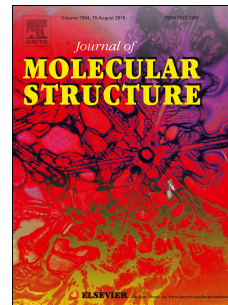


# Accepted Manuscript

Structures of (2*E*,5*E*)-2-(4-cyanobenzylidene)-5-(4-dimethylaminobenzylidene)cyclopentanone and (2*E*,5*E*)-2-benzylidene-5-cinnamylidenecyclopentanone

Christopher A. Zoto, John C. MacDonald



PII: S0022-2860(17)30811-6

DOI: [10.1016/j.molstruc.2017.06.032](https://doi.org/10.1016/j.molstruc.2017.06.032)

Reference: MOLSTR 23918

To appear in: *Journal of Molecular Structure*

Received Date: 20 March 2017

Revised Date: 7 May 2017

Accepted Date: 7 June 2017

Please cite this article as: C.A. Zoto, J.C. MacDonald, Structures of (2*E*,5*E*)-2-(4-cyanobenzylidene)-5-(4-dimethylaminobenzylidene)cyclopentanone and (2*E*,5*E*)-2-benzylidene-5-cinnamylidenecyclopentanone, *Journal of Molecular Structure* (2017), doi: 10.1016/j.molstruc.2017.06.032.

This is a PDF file of an unedited manuscript that has been accepted for publication. As a service to our customers we are providing this early version of the manuscript. The manuscript will undergo copyediting, typesetting, and review of the resulting proof before it is published in its final form. Please note that during the production process errors may be discovered which could affect the content, and all legal disclaimers that apply to the journal pertain.



**Structures of (2*E*,5*E*)-2-(4-cyanobenzylidene)-5-(4-dimethylaminobenzylidene)cyclopentanone and (2*E*,5*E*)-2-benzylidene-5-cinnamylidenecyclopentanone**

Christopher A. Zoto\*, John C. MacDonald

*Department of Chemistry and Biochemistry, Worcester Polytechnic Institute, 100 Institute Road,*

*Worcester, MA 01609, USA*

\*Email address: czoto@hotmail.com; Telephone: (508)-233-5084

*Keywords:* 2,5-diarylidene-cyclopentanone, X-ray crystal structure, DFT, crystal packing, spectroscopic, photophysical

**Abstract**

The X-ray crystal structures of (2*E*,5*E*)-2-(4-cyanobenzylidene)-5-(4-dimethylaminobenzylidene)cyclopentanone (**I**) and (2*E*,5*E*)-2-benzylidene-5-cinnamylidenecyclopentanone (**II**) are presented, compared to the gas phase structures calculated using density functional theory, and discussed in the context of the photophysical behavior exhibited by **I** and **II**. Compound **I** crystallizes in the triclinic space group  $P\bar{1}$  with  $a = 6.8743(2)$  Å,  $b = 8.8115(2)$  Å,  $c = 14.9664(4)$  Å,  $\alpha = 77.135(2)^\circ$ ,  $\beta = 81.351(2)^\circ$ ,  $\gamma = 80.975(2)^\circ$ , and  $Z = 2$ , and exhibits a planar structure. Compound **II** crystallizes in the monoclinic space group  $C2/c$  with  $a = 33.4281(10)$  Å,  $b = 11.9668(4)$  Å,  $c = 7.8031(2)$  Å,  $\beta = 92.785(2)^\circ$ , and  $Z = 8$ , and adopts a nonplanar structure in the solid state and calculated structure.

## 1. Introduction

The class of organic compounds called 2,5-diarylidene-cyclopentanones have received attention in various types of applications, including their use as fluorescent probes for solvent polarity [1], fluoroionophores [2], nonlinear optical materials [3], and photosensitizers [4]. Our previous investigations of (2*E*,5*E*)-2-(4-cyanobenzylidene)-5-(4-dimethylaminobenzylidene)cyclopentanone (**I**) [5], symmetrically-unsubstituted 2,5-diarylidene-cyclopentanones [6, 7], and alkylamino-substituted 2-arylidene- and 2,5-diarylidene-cyclopentanones [8] in solution have shown that the spectroscopic and photophysical properties of these compounds change to varying degrees with respect to solvent polarity. In particular, nonsymmetrically-substituted cyclopentanones such as compound **I** and alkylamino-substituted 2-arylidene- and 2,5-diarylidene-cyclopentanones [8] exhibit solvatochromism and photoinduced internal charge transfer (ICT) due to the push-pull effect of the electron-donating and electron-withdrawing groups through the conjugated backbone. It was demonstrated through experimental and computational work that both **I** [5] and the alkylamino-substituted 2,5-diarylidene-cyclopentanones [8] undergo photoinduced ICT. The ICT state is an excited state characterized by the transfer of electron density from the electron donor end of the molecule to the electron acceptor end of the molecule upon photoexcitation. The nature of ICT excited states gives rise to lower energies of fluorescence than the locally excited (LE) states, such that the fluorescence of an ICT state is red shifted relative to the LE state. Furthermore, we have shown that (2*E*,5*E*)-2,5-bis(4-dimethylaminobenzylidene)cyclopentanone acts as a direct photosensitizer of singlet state oxygen ( $^1\Delta_g$ ), a highly electrophilic oxygen species, and reacts with  $^1\Delta_g$  in oxygenated solutions, in addition to undergoing (*E,E*)  $\rightarrow$  (*E,Z*) photoisomerization in deoxygenated solutions [9].

Here, we present the crystal structures of two nonsymmetrically-substituted cyclopentanones, (2*E*,5*E*)-2-(4-cyanobenzylidene)-5-(4-dimethylaminobenzylidene)cyclopentanone (**I**) and (2*E*,5*E*)-2-benzylidene-5-cinnamylidenecyclopentanone (**II**), shown in Figure 1, and the corresponding structures predicted by DFT. Our previous work comparing calculated DFT structures of structurally-related substituted cyclopentanones to the corresponding experimental crystal structures has revealed that DFT generally is able to predict the LE structures of nonsymmetrically-substituted cyclopentanones quite accurately [8]. Establishing a computational method such as DFT that can predict the structures of substituted cyclopentanones reliably is important in the context of our work not only for cases where the LE structures of substituted cyclopentanones cannot be determined experimentally using X-ray diffraction, but also because knowing the structures, relative energies, and changes in the electronic distributions of  $\pi$  electrons in the molecular orbitals of ground state HOMOs and excited state LUMOs is essential for understanding both the photophysical and solvatochromic properties of substituted cyclopentanones, like that reported in [8]. This work was carried out to determine whether knowledge of the molecular structures of **I** and **II** would provide further insight toward understanding the spectroscopic and photophysical properties of these class of compounds as well as their chemical reactivity and mechanistic behavior in single- and multi-component reactions.

## 2. Experimental

All reagents and solvents were purchased from Sigma-Aldrich, Alfa Aesar, and Pharmco and were used without further purification. Purity of all intermediate and target compounds was confirmed by thin layer chromatography. The percent yields of the intermediate and target compounds were not reported at the time the synthetic workups were carried out but were found to range between moderate to high (50% - 100%). NMR spectra were obtained with a Bruker<sup>®</sup> AVANCE III 500 (500 MHz) NMR spectrometer. ATR-IR spectra were measured using a Perkin-Elmer<sup>®</sup> Spectrum One IR spectrometer.

### *Synthesis and structural characterization of compounds I and II*

Compound **I** was synthesized in two steps (Figure 2(a)). The first step involved synthesizing the precursor intermediate (*E*)-2-(4-dimethylaminobenzylidene)cyclopentanone (**IA**). Cyclopentanone (0.42 g, 5.0 mmol), 4-dimethylaminobenzaldehyde (0.75 g, 5.0 mmol), and N,N-dimethylammonium-N',N'-dimethylcarbamate (DIMCARB) (27.5 mmol, 3.7 g) in CH<sub>2</sub>Cl<sub>2</sub> (5.5 mL) were stirred for 12 hours at RT. The solvent was then removed under reduced pressure, the organic phase was extracted with CH<sub>2</sub>Cl<sub>2</sub>, and the combined organic layer extracts were dried over anhydrous sodium sulfate, filtered, and evaporated under reduced pressure. The crude product residue was purified by silica gel column chromatography using a gradient approach of hexanes/ethyl acetate, beginning with 100% hexanes, gradually increasing the eluting solvent polarity with ethyl acetate, to afford pure **IA** as a yellow solid. <sup>1</sup>H NMR (CDCl<sub>3</sub>): δ (ppm) 1.94 (p, 2H), 2.30 (t, 2H), 2.87 (td, 2H), 2.95 (s, 6H), 6.62 (d, 2H), 7.28 (s, 1H), 7.38 (d, 2H); <sup>13</sup>C NMR (CDCl<sub>3</sub>): δ (ppm) 19.1, 28.4, 28.7, 36.8, 39.1, 110.8, 122.3, 130.0, 131.5, 132.3, 149.9, 207.1.

The second step involved a base-catalyzed crossed-aldol condensation of an equimolar amount of **IA** (0.45 g, 2.1 mmol) and 4-cyanobenzaldehyde (0.27 g, 2.1 mmol) in MeOH containing 2.5 % (w/v) NaOH (0.6 mL). A red precipitate emerged immediately from the reaction mixture, which was then stirred for 12 hours at RT. The precipitate was collected by vacuum filtration, washed with cold MeOH, and then purified by silica gel column chromatography using a gradient approach of hexanes/ethyl acetate, beginning with 100% hexanes, gradually increasing the eluting solvent polarity with ethyl acetate, to afford pure **I** as a red solid. Crystals of **I** decomposed at  $\sim 260^{\circ}\text{C}$  prior to melting.  $^1\text{H NMR}$  ( $\text{CDCl}_3$ ):  $\delta$  (ppm) 2.99 (s, 6H), 3.03 (s, 4H), 6.66 (d, 2H), 7.42 (s, 1H), 7.47 (d, 2H), 7.55 (s, 1H), 7.60 (d, 2H), 7.62 (d, 2H);  $^{13}\text{C NMR}$  ( $\text{CDCl}_3$ ):  $\delta$  (ppm) 25.56, 25.61, 39.1, 110.7, 110.9, 117.7, 122.4, 128.6, 129.6, 130.5, 131.3, 132.1, 135.4, 139.7, 140.9, 150.3, 194.3. IR:  $\nu$  ( $\text{cm}^{-1}$ ) 2907, 2224, 1682, 1612, 1574, 1528, 1444, 1414, 1372, 1321, 1285, 1254, 1231, 1180, 1165, 1119, 1059, 988, 944, 828, 812.

Compound **II** was synthesized in two steps (Figure 2(b)). The first step involved synthesizing the precursor intermediate (*E*)-2-benzylidenecyclopentanone (**IIA**). Cyclopentanone (0.42 g, 5.0 mmol), benzaldehyde (0.53 g, 5.0 mmol), and DIMCARB (27.5 mmol, 3.7 g) in  $\text{CH}_2\text{Cl}_2$  (5.5 mL) were stirred for 12 hours at RT. The solvent was then removed under reduced pressure. To the residue was added 0.5 M  $\text{H}_2\text{SO}_4$  (10 mL) and extracted with ethyl acetate. The combined organic layer extracts were dried over anhydrous sodium sulfate, filtered, and evaporated under reduced pressure. The crude product residue was purified by silica gel column chromatography using a gradient approach of hexanes/ethyl acetate, beginning with 100% hexanes, gradually increasing the eluting solvent polarity with ethyl acetate, to afford pure **IIA** as a yellow solid.  $^1\text{H NMR}$  ( $\text{CDCl}_3$ ):  $\delta$  (ppm) 1.96 (p, 2H), 2.34 (t, 2H), 2.91 (td, 2H), 7.29-7.36 (m,

4H), 7.46 (d, 2H);  $^{13}\text{C}$  NMR ( $\text{CDCl}_3$ ):  $\delta$  (ppm) 20.2, 29.4, 37.8, 128.7, 129.3, 130.5, 132.3, 135.5, 136.1, 208.1.

The second step involved a base-catalyzed crossed-aldol condensation of an equimolar amount of **IIA** (0.75 g, 4.3 mmol) and (*E*)-cinnamaldehyde (0.57 g, 4.3 mmol) in EtOH containing 2.5 % (w/v) NaOH (2.0 mL). A yellow precipitate emerged immediately from the reaction mixture, which was then stirred for 14 hours at RT. The precipitate was collected by vacuum filtration, washed with cold EtOH, and dried. Recrystallization from EtOH (2x) afforded pure **II** as yellow flakes. Crystals of **II** melted at 192°C.  $^1\text{H}$  NMR ( $\text{CDCl}_3$ ):  $\delta$  (ppm) 2.85-2.92 (m, 2H), 3.00-3.05 (m, 2H), 6.92-6.94 (m, 2H), 7.24 (d, 2H), 7.30 (t, 3H), 7.37 (t, 3H), 7.44-7.46 (m, 3H), 7.52 (d, 2H).  $^{13}\text{C}$  NMR ( $\text{CDCl}_3$ ):  $\delta$  (ppm) 24.4, 26.2, 124.7, 127.3, 128.8, 129.1, 129.3, 130.7, 133.3, 135.9, 136.5, 138.5, 138.6, 141.6, 195.7. IR:  $\nu$  ( $\text{cm}^{-1}$ ) 3059, 1682, 1624, 1590, 1514, 1491, 1465, 1447, 1338, 1281, 1240, 1181, 1154, 1104, 969, 919, 894, 837.

#### *Determination of the crystal structures of I and II*

Suitable single crystals of **I** and **II** were mounted on a Bruker-AXS Kappa APEX CCD diffractometer. Diffraction data were collected at RT using graphite monochromated Mo-K $\alpha$  radiation ( $\lambda = 0.71073 \text{ \AA}$ ) by the omega-scan technique. Empirical absorption corrections were applied using the SADABS program [10]. The unit cells and space groups were determined using the SAINT+ program [11]. Structures were solved by direct methods and refined by full matrix least-squares using the SHELXTL program [12]. Refinement was based on  $F^2$  using all reflections. All non-hydrogen atoms were refined anisotropically. Hydrogen atoms on carbon atoms were all located in the difference maps and subsequently placed at idealized positions and given isotropic U values 1.2 times that of the carbon atom which they were bonded. Both

structures were refined to  $R_1$  values of  $< 5\%$ . Mercury 2.4 software was used to examine the molecular structures and crystal packing [13].

#### *Quantum chemical calculations using density functional theory*

Gaussian 09<sup>®</sup> [14] was used to perform DFT and TD-DFT calculations, carried out at the B3LYP/6-311+G(d,p) (**I**) and B3LYP/6-31G(d) (**II**) levels of theory. Geometry optimizations were carried out in the gas phase and minimum energy structures were confirmed by obtaining all positive frequencies for the calculated modes of vibration. The DFT gas phase geometry was used in all solvent calculations without further optimization. Solvent effects were computed using the Self-Consistent Reaction Field Polarizable Continuum Model (SCRF PCM) options. For TD-DFT, the first five lowest excited singlet and triplet states were calculated and the excited state orbital configurations and excited state energies were determined. Only the first three lowest excited singlet states ( $S_1$ ,  $S_2$ , and  $S_3$ , respectively) are reported in this manuscript.

### **3. Results and Discussion**

#### *Crystal structures and DFT structures of I and II*

The crystal structures and crystal packing of **I** and **II** with anisotropic displacement parameters and atomic numbering are shown in Figure 3. A summary of the crystallographic data and refinement parameters of **I** and **II** is given in Table 1. Compound **I** crystallizes in the triclinic space group  $P\bar{1}$  with  $a = 6.8743(2)$  Å,  $b = 8.8115(2)$  Å,  $c = 14.9664(4)$  Å,  $\alpha = 77.135(2)^\circ$ ,  $\beta = 81.351(2)^\circ$ ,  $\gamma = 80.975(2)^\circ$ , and  $Z = 2$ . The molecular structure of **I** is fully extended in the ( $E,E$ ) conformation and is essentially flat with the central cyclopentanone ring and phenyl rings on both ends of the molecule nearly coplanar. The torsion angles within the cyclopentanone ring are  $3.0^\circ$  ( $C_9-C_{10}-C_{11}-C_{12}$ ),  $-2.7^\circ$  ( $C_{13}-C_9-C_{10}-C_{11}$ ), and  $-2.4^\circ$  ( $C_{13}-C_{12}-C_{11}-C_{10}$ ) such that the ring is

essentially flat with the saturated carbons exhibiting no significant torsional buckling. The angles between the mean plane defined by the central cyclopentanone ring and methyl groups (C<sub>8</sub>-C<sub>14</sub>) and the mean planes of the amino-substituted and nitrile-substituted phenyl rings are 4.3° and 2.1°, respectively. Phenyl rings in dibenzylidene compounds such as **I** generally are expected to be coplanar or close to coplanar with conjugated backbone in order to promote orbital overlap and optimize conjugation throughout the  $\pi$  system. For example, the cyclopentanone and phenyl rings in the crystal structure of the unsubstituted analogue of **I**, (2*E*,5*E*)-2,5-dibenzylidenecyclopentanone, are coplanar with no torsional distortion along the conjugated backbone [15]. Similar to that structure, eclipsing of the methylene groups on the cyclopentanone ring in **I** allows the phenyl rings to remain coplanar by minimizing repulsive interactions between the methylene hydrogen atoms and ortho hydrogen atoms on the phenyl rings, as shown in the space-filling model on the left in Figure 3c.

Molecules of **I** pack at van der Waals separation in the unit cell with no short contacts of consequence. Molecules stack on top of one another along the *b* axis, [010], where alternating molecules within stacks are related by inversion (Figure 3d). That packing arrangement positions the dimethylamino-substituted phenyl ring over the cyano-substituted phenyl ring of adjacent neighbors within a stack, as shown in Figure 3e. Alternate stacking of electron-rich and electron-deficient phenyl rings overlapping at a separation of 3.6 Å suggests that  $\pi$  donor-acceptor interactions between the lowest-energy empty molecular orbital (LUMO) and highest-energy filled molecular orbital (HOMO) of **I** should play a role influencing molecular aggregation during nucleation of crystals to favor centrosymmetric packing. Shown in Figure 4 are the molecular orbitals for the LUMO and HOMOs of compound **I** calculated using TD-DFT. Taking into consideration that the LUMO ( $\pi^*$ ) resides predominantly on the cyclopentanone and cyano-

substituted phenyl rings, and the HOMO ( $\pi$ ) resides predominantly on the cyclopentanone and dimethylamino-substituted phenyl ring, it is not surprising to observe that adjacent molecules of **I** adopt a centrosymmetric packing arrangement at least in part to maximize favorable overlap between the LUMO and HOMO. Kitaigorodski also has shown that molecules related via a center of symmetry usually pack more efficiently compared to molecules related by other symmetry operators [16].

As shown in Table 2, comparison of the molecular geometries obtained from the experimental crystal structure and the calculated DFT ground state structure shows good agreement between bond lengths and bond angles as a whole. Differences between experimental and calculated bond lengths varied between 0.001 Å – 0.023 Å and bond angles between 0.01° – 3.5°. The calculated DFT geometry for **I** predicts a planar conjugated backbone and both phenyl rings rotated out of the plane of the central cyclopentanone ring by just 6° such that the conformation of DFT structure is consistent with that of the crystal structure. That geometry also is consistent with the structures of symmetrically-disubstituted cyclopentanones determined previously using DFT calculations [8].

Compound **II** crystallizes in the monoclinic space group  $C2/c$  with  $a = 33.4281(10)$  Å,  $b = 11.9668(4)$  Å,  $c = 7.8031(2)$  Å,  $\beta = 92.785(2)^\circ$ , and  $Z = 8$ . As shown on the right in Figure 3, the molecular structure of **II** has a twisted rather than planar conformation with both phenyl rings rotating out of the plane of the conjugated backbone. The mean planes of the phenyl rings in the benzylidene and cinnamylidene substituents rotate significantly out of the mean plane defined by the central cyclopentanone and acyclic carbon atoms ( $C_1$ - $C_8$  and  $C_{15}$ ) by 43.6° and 20.6°, respectively. The torsion angles within the cyclopentanone ring are  $-20.1^\circ$  ( $C_1$ - $C_2$ - $C_3$ - $C_4$ ),  $-17.5^\circ$

(C<sub>1</sub>-C<sub>5</sub>-C<sub>4</sub>-C<sub>3</sub>), and 22.8° (C<sub>2</sub>-C<sub>3</sub>-C<sub>4</sub>-C<sub>5</sub>), reflecting significant buckling of the central ring. The mean planes of the phenyl groups on either end are twisted with respect to one another by 59.3°.

Considering that compound **II** contains no obvious structural features that might cause repulsive steric interactions, major twisting of the phenyl ring on the benzylidene substituent likely is due to intermolecular interactions caused by crystal packing. Molecules pack at van der Waals separation in the unit cell with no intermolecular contacts less than the VDW contact distances. The molecules stack with alternating molecules related by glide symmetry along the *c* axis, [001], as shown in Figure 3d. Within a stack, molecules align in parallel positioned with the benzylidene groups overlapping and the cinnamylidene groups overlapping. Phenyl rings on the benzylidene substituents align edge-to-face forming a C-H $\cdots$  $\pi$  interaction involving C<sub>17</sub>-H<sub>17</sub> on one phenyl group pointing toward the  $\pi$  cloud on an adjacent ring, C<sub>16</sub>-C<sub>21</sub>, as shown in Figure 3e. The contact distances of C<sub>17</sub> $\cdots$ centroid of ring = 3.9 Å and H<sub>17</sub> $\cdots$ centroid of ring = 3.1 Å are consistent with C-H $\cdots$  $\pi$  edge-to-face interactions observed in the crystal structure of benzene [17]. That type of intermolecular interaction is energetically favorable and is commonly observed when aromatic ring systems pack in crystalline solids [18]. For example, Marjani has reported that the 4-aminophenyl group in the crystal structure of N-(2-pyridylmethylene)benzene-1,4-diamine twists 25° out of the molecular plane to form C-H $\cdots$  $\pi$  interactions with adjacent molecules [19].

Comparison between the geometry of **II** in the crystalline state and its calculated DFT geometry shows reasonable agreement in the bond lengths and bond angles, as shown in Table 3. Similar to the structure of **I**, differences between experimental and calculated bond lengths varied between 0.001 Å – 0.023 Å with bond angles varying between 0.01° – 3.5°. Notably, the phenyl substituents in the DFT structure exhibit far less twisting, rotating just ~10° out of the

mean plane of the central cyclopentanone ring, which supports our hypothesis that greater twisting of the phenyl groups in the solid state is due largely to effects of crystal packing and, in the case of the benzylidene group, formation of a C-H $\cdots\pi$  interaction. Close examination of the X-ray and DFT bond lengths in the carbon backbone reveals an interesting trend. The DFT values for double bonds (C<sub>5</sub>-C<sub>6</sub>, C<sub>7</sub>-C<sub>8</sub>, and C<sub>2</sub>-C<sub>15</sub>) in the valence bond structure of **II** (Figure 1) are longer by 0.004-0.023 Å than the corresponding bonds in the crystal structure, while the DFT values for single bonds (C<sub>6</sub>-C<sub>7</sub> and C<sub>15</sub>-C<sub>16</sub>) in the valence bond structure are shorter by 0.001-0.004 than the corresponding bonds in the crystal structure. Although the magnitude of the differences in those bond lengths is small, the trend of alternating longer C=C and shorter C-C bonds suggests that the DFT structure exhibits bond orders with a higher degree of conjugation in the carbon backbone compared to the crystal structure. That finding is consistent with the conformation of **II** exhibiting greater deviation from planarity in the crystalline solid, where rotation of the phenyl rings and buckling of the central cyclopentanone ring should inhibit optimal overlap of p orbitals along the central  $\pi$  system. It is interesting to note that the bond lengths for compound **I** (Table 2) do not show the same trend of alternating shorter C=C and longer C-C bond lengths for the DFT values, which makes sense given the close structural similarity and nearly planar conformations of the DFT and crystal structures of **I**.

#### *Photophysical properties of compounds I and II*

Knowledge of the structures of these compounds provides some degree of insight to understanding the spectroscopic and photophysical properties exhibited by **I** and **II**. Structural features such as polyene chain length and the presence of electron-donating and electron-withdrawing groups have been shown to effect the spectroscopic and photophysical properties for this class of compounds. Compound **I** is an example of a “donor-acceptor-acceptor” molecule

that we previously have demonstrated exhibits solvatochromism and photoinduced internal charge transfer (ICT) [5] resulting from the presence of the strongly electron-donating dimethylamino group and the strongly electron-withdrawing cyano group on opposite ends of the conjugated carbon backbone. Figure 5 shows absorption and fluorescence spectra of **I** at room temperature in methanol, chloroform, and carbon tetrachloride. We found that **I** undergoes bathochromic (red) shifts as solvent polarity increases as indicated by the shifts in absorption maxima from 446 nm (carbon tetrachloride) to 473 nm (methanol) and fluorescence maxima from 513 nm (carbon tetrachloride) to 693 nm (methanol). Shown in Figure 4, the computed molecular orbitals of **I** reveal the ICT ( $\pi$ ,  $\pi^*$ ) nature of the  $S_1$  excited state, where  $\pi$  electron density is transferred from the HOMO ( $\pi$ ) on the side bearing the dimethylamino group to the LUMO ( $\pi^*$ ) on the side bearing the cyano group upon photoexcitation. The HOMO-2 (n) orbital was determined to be a nonbonding orbital centered on the carbonyl group. Although we have studied the photophysical behavior of **I** only in solution and not in the solid state, the similarity in the molecular structure of **I** both in the solid state (crystal structure) and in the gas phase (calculated DFT structure) suggest that the observed planar structure of compound **I** is the lowest energy conformation. Therefore, it is reasonable to expect that molecular structure predominates in solution and represents the most stable ground state conformation giving rise to the photophysical behavior we have observed.

In contrast to **I**, compound **II** contains unsubstituted phenyl moieties and exhibits a smaller degree of ICT due to the absence of strongly electron-donating and electron-withdrawing groups. As depicted in Figure 4, the computed molecular orbitals of **II** show that in the HOMO ( $\pi$ ),  $\pi$  electron density resides largely on the cinnamylidene group. Upon photoexcitation to the  $S_1$  state,  $\pi$  electron density in the LUMO ( $\pi^*$ ) shifts slightly onto the conjugated backbone and

carbonyl group in the center of the molecule rather than transferring completely to the opposite side as in compound **I**. Our previous studies of the spectroscopic properties of **II** in various solvents (Figure 6) showed that **II** fluoresces only in protic solvents such as alcohols and acetic acid in which photoexcitation from  $S_0$  to  $S_1$  involve  $\pi$  to  $\pi^*$  transitions rather than  $n$  to  $\pi^*$  transitions [20]. Nonpolar solvents that were unable to induce fluorescence upon photoexcitation necessarily involved  $n$  to  $\pi^*$  transitions where the absence of fluorescence from  $S_1$  is attributed to efficient intersystem crossing of the singlet  $\pi^*$  states to triplet  $\pi^*$  states in accordance to El-Sayed's rule [21]. We have demonstrated similar photophysical behavior previously for a related family of three symmetrically unsubstituted 2,5-diarylidene-cyclopentanones [22]. As with **I**, we have studied the photophysical properties of compound **II** only in solution and not in the solid state. Our finding that the structure is nonplanar both in the solid state (crystal structure) and the gas phase (calculated DFT structure) indicate that molecules of **II** will adopt a twisted structure in solution. Given the discrepancies between the crystal and calculated structures with regard to the degree of rotation of the phenyl substituents and buckling present in the cyclopentanone ring, we can conclude only that the lowest energy conformation likely also is nonplanar in solution in the ground state.

TD-DFT spectral calculations were carried out both in the gas phase and in solvent, employing the SCRF PCM method. Table 4 shows the TD-DFT calculations for the first three lowest lying excited singlet states ( $S_1$ ,  $S_2$ , and  $S_3$ , respectively) in the gas phase and in solvent (chloroform for **I** and ethanol for **II**). Direct comparison between the experimental UV-Visible absorption spectra, plotted together with the TD-DFT calculations are shown in Figure 7. For **I**, the  $S_0 \rightarrow S_1$  transition was observed at 468 nm in chloroform and is predicted by TD-DFT to be a strong transition appearing at 473 nm in the gas phase and 515 nm in chloroform, arising from

the HOMO ( $\pi$ )  $\rightarrow$  LUMO ( $\pi^*$ ) orbital configuration. The  $S_0 \rightarrow S_2$  transition is computed to be a forbidden  $n \rightarrow \pi^*$  excitation arising from the HOMO-2 ( $n$ )  $\rightarrow$  LUMO ( $\pi^*$ ), where HOMO-2 is nonbonding orbital localized on the carbonyl oxygen atom. The calculated wavelengths are 426 nm in the gas phase and 403 nm in chloroform. Absorption to the  $S_2$  state has not been observed owing to its forbidden nature. Excitation to  $S_3$  is predicted to occur at 367 nm in the gas phase and 376 nm in chloroform with major Configuration Interaction (CI) configurations HOMO-1  $\rightarrow$  LUMO and HOMO  $\rightarrow$  LUMO + 1, corresponding to a  $\pi \rightarrow \pi^*$  transition delocalized over the entire molecule. The band observed at  $\lambda_{\text{max}} = 322$  nm is assigned to this computed excitation.

For **II**, in the gas phase, the  $S_0 \rightarrow S_1$  excitation was predicted by TD-DFT to be a forbidden ( $n, \pi^*$ ) state in the gas phase with a calculated transition energy of  $23,041 \text{ cm}^{-1}$  ( $\lambda$  434 nm) and HOMO-2  $\rightarrow$  LUMO as the major CI configuration. The  $S_0 \rightarrow S_2$  excitation was predicted to be a spin allowed ( $\pi, \pi^*$ ) state with a calculated transition energy of  $25,316 \text{ cm}^{-1}$  ( $\lambda$  395 nm), and with HOMO  $\rightarrow$  LUMO as the major CI configuration. Lastly, the  $S_0 \rightarrow S_3$  excitation was also predicted to be ( $\pi, \pi^*$ ), with a calculated transition energy of  $28,736 \text{ cm}^{-1}$  ( $\lambda$  348 nm), with HOMO-1  $\rightarrow$  LUMO as the major CI configuration. In ethanol, the lowest lying  $^1(\pi, \pi^*)$  state shifts below that of  $^1(n, \pi^*)$ , making it the  $S_1$  state, thereby inducing fluorescence, as was experimentally observed (Figure 6). From TD-DFT, calculated transition energies for  $S_1$ ,  $S_2$ , and  $S_3$  were  $23,810 \text{ cm}^{-1}$  ( $\lambda$  420 nm),  $24,390 \text{ cm}^{-1}$  ( $\lambda$  410 nm), and  $28,329 \text{ cm}^{-1}$  ( $\lambda$  353 nm).

## Conclusions

The single crystal X-ray structures of two 2,5-diarylidene cyclopentanone compounds have been measured and solved by X-Ray Diffractometry. Excellent agreement was established between the experimental single crystal X-ray structure and the predicted DFT structure of **I** and

**II** in both bond lengths and bond angles. The single crystal X-ray structure of **I** was found to be mainly planar, with angles between the mean plane defined by the central cyclopentanone ring and methyl groups (C<sub>8</sub>-C<sub>14</sub>) and the mean planes of the amino-substituted and nitrile-substituted phenyl rings of 4.3° and 2.1°, respectively. Alternate stacking of electron-rich and electron-deficient phenyl rings overlapping at a separation of 3.6 Å suggests that  $\pi$  donor-acceptor interactions between the LUMO and HOMO should play a role of influencing molecular aggregation during nucleation of crystals to favor centrosymmetric packing. The single crystal X-ray structure of **II** was found to be nonplanar, with mean planes of the phenyl rings in the benzylidene and cinnamylidene ends of the molecule rotating out of the mean plane defined by the central cyclopentanone ring and acyclic carbon atoms (C<sub>1</sub>-C<sub>8</sub> and C<sub>15</sub>) by 43.6° and 20.6°, respectively. The mean planes of the phenyl groups on either end are twisted with respect to one another by 59.3°. Furthermore, surveys of the spectroscopic, photophysical, and reactivity properties of these compounds show and explain how molecular structure plays an important role in determining the outcomes of these properties.

### Supporting Information Available

The Crystallographic Information Files (CIFs) for both compounds **I** and **II** are provided in the Supplementary Information. The crystallographic data is from The Cambridge Crystallographic Data Centre (CCDC), 12 Union Road, Cambridge CB2 1EZ, UK, Fax: +44(0)1223-336033.

**References**

- [1] (a) V. G. Pivovarenko, A. V. Klueva, A. O. Doroshenko, A. P. Demchenko, *Chem. Phys. Lett.* 325 (2000) 389.  
(b) P. K. Das, R. Pramanik, D. Banerjee, S. Bagchi, *Spectrochim. Acta A* 56 (2000) 2763.
- [2] A. O. Doroshenko, A. V. Grigorovich, E. A. Posokhov, V. G. Pivovarenko, A. P. Demchenko, *Mol. Eng.* 8 (1999) 199.
- [3] (a) J. Kawamata, K. Inoue, T. Inabe, *Bull. Chem. Soc. Jpn.* 71 (1998) 2777.  
(b) P. Kaatz, D. P. Shelton, *J. Chem. Phys.* 105 (1996) 3918.  
(c) W. Tao, W. Fei-peng, S. Men-quan, *Chem. Res. Chin. Univ.* 19 (2003) 470.
- [4] (a) M. V. Barnabus, A. Liu, A. D. Trifunac, V. V. Krongauz, C. T. Chang, *J. Phys. Chem.* 96 (1992) 212.  
(b) T. J. Dougherty, C. J. Gomer, B. W. Henderson, G. Jori, O. Kessel, M. Korbelik, J. Moan, Q. Peng, *J. Natl. Cancer. Inst.* 90 (1998) 889.
- [5] C. A. Zoto, R. E. Connors, *J. Mol. Struct.* 982 (2010) 121.
- [6] R. E. Connors, M. G. Ucak-Astarlioglu, *J. Phys. Chem. A* 107 (2003) 7684.
- [7] M. G. Ucak-Astarlioglu, R. E. Connors, *J. Phys. Chem. A* 109 (2005) 8275.
- [8] C. A. Zoto, M. G. Ucak-Astarlioglu, J. C. MacDonald, R. E. Connors, *J. Mol. Struct.* 1112 (2016) 97.
- [9] C. A. Zoto, M. G. Ucak-Astarlioglu, R. E. Connors, *J. Mol. Struct.* 1105 (2016) 396.
- [10] SADABS; Bruker AXS Inc.: Madison, WI.
- [11] Bruker, SAINT (Version 6.14).
- [12] SHELXTL (Version 6.14) for WNT/2003; Bruker AXS Inc.: Madison, WI, 1999.
- [13] CCDC. Mercury 2.4; CCDC: Cambridge, U. K., 2009.
- [14] Gaussian 09, Revision A.02, M. J. Frisch, G. W. Trucks, H. B. Schlegel, G. E. Scuseria, M. A. Robb, J. R. Cheeseman, G. Scalmani, V. Barone, B. Mennucci, G. A. Petersson, H. Nakatsuji, M. Caricato, X. Li, H. P. Hratchian, A. F. Izmaylov, J. Bloino, G. Zheng, J. L. Sonnenberg, M. Hada, M. Ehara, K. Toyota, R. Fukuda, J. Hasegawa, M. Ishida, T. Nakajima, Y. Honda, O. Kitao, H. Nakai, T. Vreven, J. A. Montgomery, Jr., J. E. Peralta, F. Ogliaro, M. Bearpark, J. J. Heyd, E. Brothers, K. N. Kudin, V. N. Staroverov, R. Kobayashi, J. Normand, K. Raghavachari, A. Rendell, J. C. Burant, S. S. Iyengar, J. Tomasi, M. Cossi, N. Rega, J. M. Millam, M. Klene, J. E. Knox, J. B. Cross, V. Bakken, C. Adamo, J. Jaramillo, R. Gomperts, R. E. Stratmann, O. Yazyev, A. J. Austin, R. Cammi, C. Pomelli, J. W. Ochterski, R. L. Martin, K. Morokuma, V. G. Zakrzewski, G. A. Voth, P. Salvador, J. J. Dannenberg, S. Dapprich, A. D.

- Daniels, O. Farkas, J. B. Foresman, J. V. Ortiz, J. Cioslowski, and D. J. Fox, Gaussian, Inc., Wallingford CT, 2009.
- [15] C. R. Theocharis, W. Jones, J. M. Thomas, M. Motevalli, M. B. Hursthouse, *J. Chem. Soc. Perkin Trans. II* (1984) 71.
- [16] A. I. Kitaigorodskii, *Molecular Crystals and Molecules*, Academic Press, New York, 1973.
- [17] G. E. Bacon, N. A. Curry, S. A. Wilson, *Proc. R. Soc. London, Ser. A* 279 (1964) 98.
- [18] J. L. Atwood, J. W. Steed, *Encyclopedia of Supramolecular Chemistry*, Marcel Dekker, New York, 2004.
- [19] K. Marjani, M. Mousavi, F. Namazian, *J. Chem. Crystallogr.* 41 (2011) 1451.
- [20] C. A. Zoto, Structural and Photophysical Properties of Internal Charge Transfer 2-Arylidene and 2,5-Diarylidene Cyclopentanones, Ph. D. Dissertation, Worcester Polytechnic Institute, 2012.
- [21] M. A. El-Sayed, *J. Chem. Phys.* 38 (1963) 2834.
- [22] R. E. Connors, M. G. Ucak-Astarlioglu, *J. Phys. Chem. A* 107 (2003) 7684.

### Figure Captions

**Fig. 1.** Chemical structures of compounds **I** and **II**.

**Fig. 2.** Reaction schemes for the syntheses of (a) **I** and (b) **II**.

**Fig. 3.** Views of the crystal structures of compounds **I** (left) and **II** (right) showing the molecular structures viewed (a) from above and (b) edge-on with anisotropic displacement parameters at the 50% probability level, (c) space-filling models of the molecular structures, (d and e) crystal packing. The green sphere indicates the centroid of the C<sub>16</sub>-C<sub>21</sub> phenyl ring in **II**.

**Fig. 4.** Molecular orbitals of **I** and **II** computed by TD-DFT.

**Fig. 5.** Absorption spectra (left) and fluorescence spectra (right) of compound **I** in (a) methanol, (b) chloroform, and (c) carbon tetrachloride.

**Fig. 6.** Absorption spectra (left) and fluorescence spectra (right) of **II** in (a) glacial acetic acid, (b) methanol, (c) ethanol, (d) 1-propanol, (e) 2-propanol, and (f) 1-butanol.

**Fig. 7.** Experimental absorption spectra of (a) **I** (in chloroform) and (b) **II** (in ethanol) plotted together with the TD-DFT calculated results. The forbidden <sup>1</sup>(n, π\*) state is represented by the filled diamond.

**Table Captions**

**Table 1.** Crystallographic data and refinement parameters for compounds **I** and **II**.

**Table 2.** Comparison of geometries for compound **I** determined by X-ray diffraction in the solid state and by DFT calculations (B3LYP/6-31G(d) level of theory) in the gas phase.  $\Delta$  indicates the difference between corresponding geometric values determined by X-ray and DFT (X-ray–DFT).

**Table 3.** Comparison of geometries for compound **II** determined by X-ray diffraction in the solid state and by DFT calculations (B3LYP/6-31G(d) level of theory) in the gas phase.  $\Delta$  indicates the difference between corresponding geometric values determined by X-ray and DFT (X-ray–DFT).

**Table 4.** TD-DFT spectral calculations of  $S_1$ ,  $S_2$ , and  $S_3$  in gas and solvent (chloroform for **I** and ethanol for **II**).\*

Crystal Form	Compound	
	I	II
Formula	C <sub>22</sub> H <sub>20</sub> N <sub>2</sub> O	C <sub>21</sub> H <sub>18</sub> O
Formula weight (g mol <sup>-1</sup> )	328.40	286.35
Crystal system	Triclinic	Monoclinic
Space group	P-1	C2/c
Color and habit	Red, needles	Yellow, needles
Crystal size	0.05 mm × 0.20 mm × 0.50 mm	0.15 mm × 0.20 mm × 1.00 mm
a (Å)	6.8743(2)	33.4281(10)
b (Å)	8.8115(2)	11.9668(4)
c (Å)	14.9664(4)	7.8031(2)
α (°)	77.135(2)	90.00
β (°)	81.351(2)	92.785(2)
γ (°)	80.975(2)	90.00
Volume (Å <sup>3</sup> )	866.56(4)	3117.77(16)
Z	2	8
λ (Å)	0.71073	0.71073
ρ <sub>calc</sub> (g cm <sup>-3</sup> )	1.259	1.220
Temperature (K)	296(2)	296(2)
F (000)	348	1216
θ range for data collection (°)	2.39 – 28.47	1.22 – 28.30
Ranges of Miller indices	-9 ≤ h ≤ 9 -11 ≤ k ≤ 11 -20 ≤ l ≤ 19	-44 ≤ h ≤ 44 -15 ≤ k ≤ 15 -10 ≤ l ≤ 9
Absorption Coefficient (mm <sup>-1</sup> )	0.078	0.073
Reflections collected	16663	23582
Independent reflections	4370 [R <sub>int</sub> = 0.0279]	3876 [R <sub>int</sub> = 0.0275]
Reflections [I > 2σ(I)]	2395	2519
Data/restraints/parameters	4370/0/228	3876/0/200
Goodness of fit on F <sup>2</sup>	1.004	1.023
R (all data)	R <sub>1</sub> = 0.0496 wR <sub>2</sub> = 0.1460	R <sub>1</sub> = 0.0414 wR <sub>2</sub> = 0.1112

Bond Lengths (Å)			
	X-ray	DFT	$\Delta$
C <sub>1</sub> -C <sub>2</sub>	1.440(3)	1.429	0.011
C <sub>1</sub> -N <sub>1</sub>	1.131(3)	1.156	-0.025
C <sub>2</sub> -C <sub>3</sub>	1.383(3)	1.403	-0.020
C <sub>2</sub> -C <sub>7</sub>	1.383(3)	1.403	-0.020
C <sub>3</sub> -C <sub>4</sub>	1.363(3)	1.385	-0.022
C <sub>4</sub> -C <sub>5</sub>	1.396(3)	1.410	-0.014
C <sub>5</sub> -C <sub>6</sub>	1.394(3)	1.410	-0.016
C <sub>5</sub> -C <sub>8</sub>	1.453(2)	1.459	-0.006
C <sub>6</sub> -C <sub>7</sub>	1.374(3)	1.386	-0.012
C <sub>8</sub> -C <sub>9</sub>	1.336(2)	1.347	-0.011
C <sub>9</sub> -C <sub>10</sub>	1.498(2)	1.507	-0.009
C <sub>9</sub> -C <sub>13</sub>	1.485(2)	1.500	-0.015
C <sub>10</sub> -C <sub>11</sub>	1.545(2)	1.557	-0.012
C <sub>11</sub> -C <sub>12</sub>	1.500(2)	1.508	-0.008
C <sub>12</sub> -C <sub>13</sub>	1.467(3)	1.480	-0.013
C <sub>12</sub> -C <sub>14</sub>	1.343(2)	1.355	-0.012
C <sub>13</sub> -O <sub>1</sub>	1.227(2)	1.222	0.005
C <sub>14</sub> -C <sub>15</sub>	1.441(2)	1.447	-0.006
C <sub>15</sub> -C <sub>16</sub>	1.398(2)	1.411	-0.013
C <sub>15</sub> -C <sub>20</sub>	1.399(3)	1.411	-0.012
C <sub>16</sub> -C <sub>17</sub>	1.371(3)	1.382	-0.011
C <sub>17</sub> -C <sub>18</sub>	1.401(3)	1.416	-0.015
C <sub>18</sub> -C <sub>19</sub>	1.397(3)	1.416	-0.019
C <sub>18</sub> -N <sub>2</sub>	1.372(3)	1.377	-0.005
C <sub>19</sub> -C <sub>20</sub>	1.374(3)	1.383	-0.009
C <sub>21</sub> -N <sub>2</sub>	1.453(3)	1.455	-0.002
C <sub>22</sub> -N <sub>2</sub>	1.436(4)	1.455	-0.019

Dihedral Angles (°)		
	X-ray	DFT
C <sub>10</sub> -C <sub>9</sub> -C <sub>5</sub> -C <sub>6</sub>	-3.8	7.1
C <sub>11</sub> -C <sub>12</sub> -C <sub>15</sub> -C <sub>20</sub>	1.2	4.6

Bond Angles (°)			
	X-ray	DFT	$\Delta$
C <sub>1</sub> -C <sub>2</sub> -C <sub>3</sub>	121.0(2)	120.4	0.6
C <sub>1</sub> -C <sub>2</sub> -C <sub>7</sub>	119.8(2)	120.2	-0.4
C <sub>2</sub> -C <sub>1</sub> -N <sub>1</sub>	178.0(3)	179.9	-1.9
C <sub>2</sub> -C <sub>3</sub> -C <sub>4</sub>	119.8(2)	119.8	-0.01
C <sub>2</sub> -C <sub>7</sub> -C <sub>6</sub>	120.8(2)	120.3	0.5
C <sub>3</sub> -C <sub>2</sub> -C <sub>7</sub>	119.2(2)	119.4	-0.2
C <sub>3</sub> -C <sub>4</sub> -C <sub>5</sub>	122.1(2)	121.7	0.4
C <sub>4</sub> -C <sub>5</sub> -C <sub>6</sub>	117.4(2)	117.6	-0.2
C <sub>4</sub> -C <sub>5</sub> -C <sub>8</sub>	118.5(1)	117.8	0.7
C <sub>5</sub> -C <sub>6</sub> -C <sub>7</sub>	120.6(2)	121.2	-0.6
C <sub>5</sub> -C <sub>8</sub> -C <sub>9</sub>	132.1(1)	130.9	1.2
C <sub>6</sub> -C <sub>5</sub> -C <sub>8</sub>	124.2(1)	124.6	-0.4
C <sub>8</sub> -C <sub>9</sub> -C <sub>10</sub>	132.4(1)	131.6	0.8
C <sub>8</sub> -C <sub>9</sub> -C <sub>13</sub>	118.8(1)	119.3	-0.5
C <sub>9</sub> -C <sub>10</sub> -C <sub>11</sub>	106.5(1)	106.3	0.2
C <sub>9</sub> -C <sub>13</sub> -C <sub>12</sub>	108.9(1)	107.9	1.0
C <sub>9</sub> -C <sub>13</sub> -O <sub>1</sub>	124.7(1)	125.2	-0.5
C <sub>10</sub> -C <sub>9</sub> -C <sub>13</sub>	108.8(1)	109.1	-0.3
C <sub>10</sub> -C <sub>11</sub> -C <sub>12</sub>	106.6(1)	106.1	0.5
C <sub>11</sub> -C <sub>12</sub> -C <sub>13</sub>	109.1(1)	109.7	-0.6
C <sub>11</sub> -C <sub>12</sub> -C <sub>14</sub>	131.8(1)	130.7	1.1
C <sub>12</sub> -C <sub>13</sub> -O <sub>1</sub>	126.5(1)	126.9	-0.4
C <sub>12</sub> -C <sub>14</sub> -C <sub>15</sub>	132.7(1)	131.6	1.1
C <sub>13</sub> -C <sub>12</sub> -C <sub>14</sub>	119.1(1)	119.5	-0.4
C <sub>14</sub> -C <sub>15</sub> -C <sub>16</sub>	118.4(1)	118.3	0.1
C <sub>14</sub> -C <sub>15</sub> -C <sub>20</sub>	125.7(1)	125.4	0.3
C <sub>15</sub> -C <sub>16</sub> -C <sub>17</sub>	122.7(2)	122.6	0.1
C <sub>15</sub> -C <sub>20</sub> -C <sub>19</sub>	122.0(2)	122.0	0.01
C <sub>16</sub> -C <sub>15</sub> -C <sub>20</sub>	115.9(2)	116.2	-0.3
C <sub>16</sub> -C <sub>17</sub> -C <sub>18</sub>	121.0(2)	120.8	0.2
C <sub>17</sub> -C <sub>18</sub> -C <sub>19</sub>	116.8(2)	117.0	-0.2
C <sub>17</sub> -C <sub>18</sub> -N <sub>2</sub>	121.0(2)	121.5	-0.5
C <sub>18</sub> -C <sub>19</sub> -C <sub>20</sub>	121.7(2)	121.4	0.3
C <sub>18</sub> -N <sub>2</sub> -C <sub>21</sub>	120.6(2)	120.0	0.6
C <sub>18</sub> -N <sub>2</sub> -C <sub>22</sub>	120.9(2)	120.2	0.7
C <sub>19</sub> -C <sub>18</sub> -N <sub>2</sub>	122.2(2)	121.5	0.7
C <sub>21</sub> -N <sub>2</sub> -C <sub>22</sub>	118.2(2)	118.8	-0.6

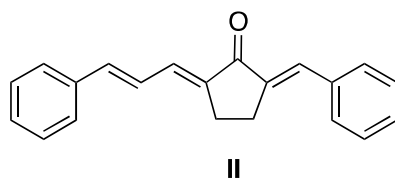
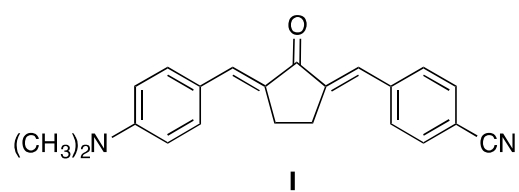
Bond Lengths (Å)			
	X-ray	DFT	$\Delta$
C <sub>1</sub> -C <sub>2</sub>	1.490(2)	1.493	-0.003
C <sub>1</sub> -C <sub>5</sub>	1.478(2)	1.484	-0.006
C <sub>1</sub> -O <sub>1</sub>	1.225(2)	1.227	-0.002
C <sub>2</sub> -C <sub>3</sub>	1.504(2)	1.512	-0.008
C <sub>2</sub> -C <sub>15</sub>	1.336(2)	1.351	-0.015
C <sub>3</sub> -C <sub>4</sub>	1.541(2)	1.560	-0.019
C <sub>4</sub> -C <sub>5</sub>	1.503(2)	1.510	-0.007
C <sub>5</sub> -C <sub>6</sub>	1.336(2)	1.354	-0.018
C <sub>6</sub> -C <sub>7</sub>	1.440(2)	1.439	0.001
C <sub>7</sub> -C <sub>8</sub>	1.333(2)	1.356	-0.023
C <sub>8</sub> -C <sub>9</sub>	1.463(2)	1.460	0.003
C <sub>9</sub> -C <sub>10</sub>	1.388(2)	1.409	-0.021
C <sub>9</sub> -C <sub>14</sub>	1.395(2)	1.410	-0.015
C <sub>10</sub> -C <sub>11</sub>	1.383(2)	1.393	-0.010
C <sub>11</sub> -C <sub>12</sub>	1.374(3)	1.396	-0.022
C <sub>12</sub> -C <sub>13</sub>	1.376(2)	1.399	-0.023
C <sub>13</sub> -C <sub>14</sub>	1.378(2)	1.390	-0.012
C <sub>15</sub> -C <sub>16</sub>	1.464(2)	1.460	0.004
C <sub>16</sub> -C <sub>17</sub>	1.397(2)	1.411	-0.014
C <sub>16</sub> -C <sub>21</sub>	1.395(2)	1.411	-0.016
C <sub>17</sub> -C <sub>18</sub>	1.382(2)	1.391	-0.009
C <sub>18</sub> -C <sub>19</sub>	1.379(2)	1.397	-0.018
C <sub>19</sub> -C <sub>20</sub>	1.377(2)	1.397	-0.020
C <sub>20</sub> -C <sub>21</sub>	1.381(2)	1.393	-0.012

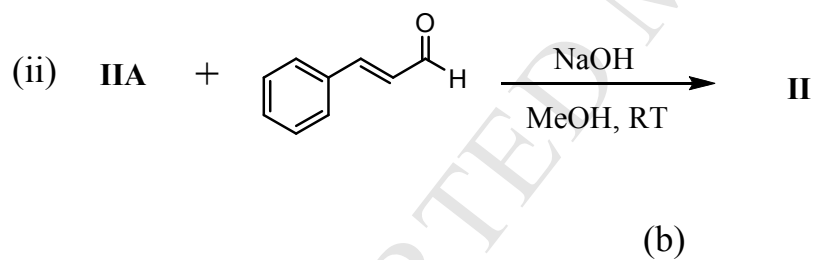
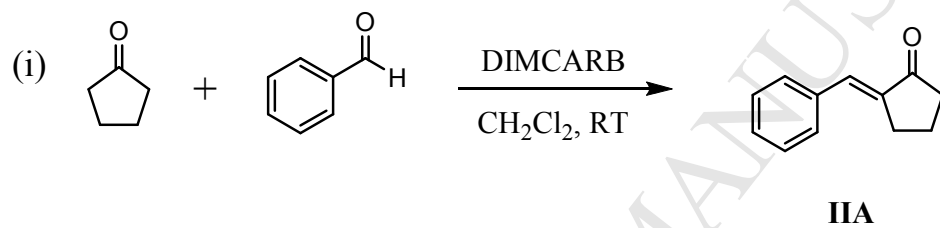
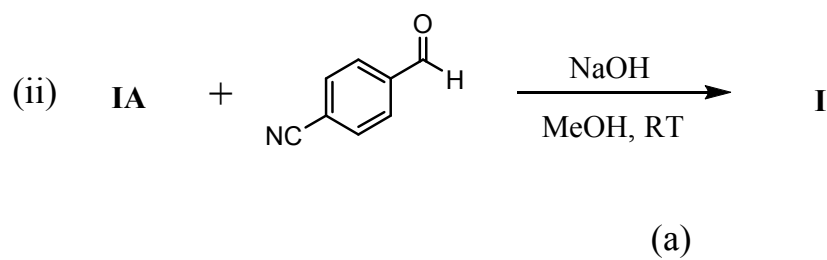
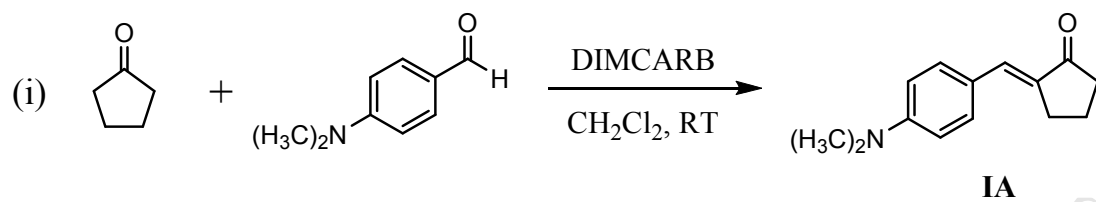
Dihedral Angles (°)		
	X-ray	DFT
C <sub>1</sub> -C <sub>2</sub> -C <sub>3</sub> -C <sub>4</sub>	-20.1	9.9
C <sub>1</sub> -C <sub>5</sub> -C <sub>4</sub> -C <sub>3</sub>	-17.5	10.3
C <sub>21</sub> -C <sub>16</sub> -C <sub>9</sub> -C <sub>14</sub>	52.8	-15.4
C <sub>4</sub> -C <sub>6</sub> -C <sub>9</sub> -C <sub>14</sub>	12.9	-1.1
C <sub>3</sub> -C <sub>15</sub> -C <sub>16</sub> -C <sub>21</sub>	35.0	-9.7

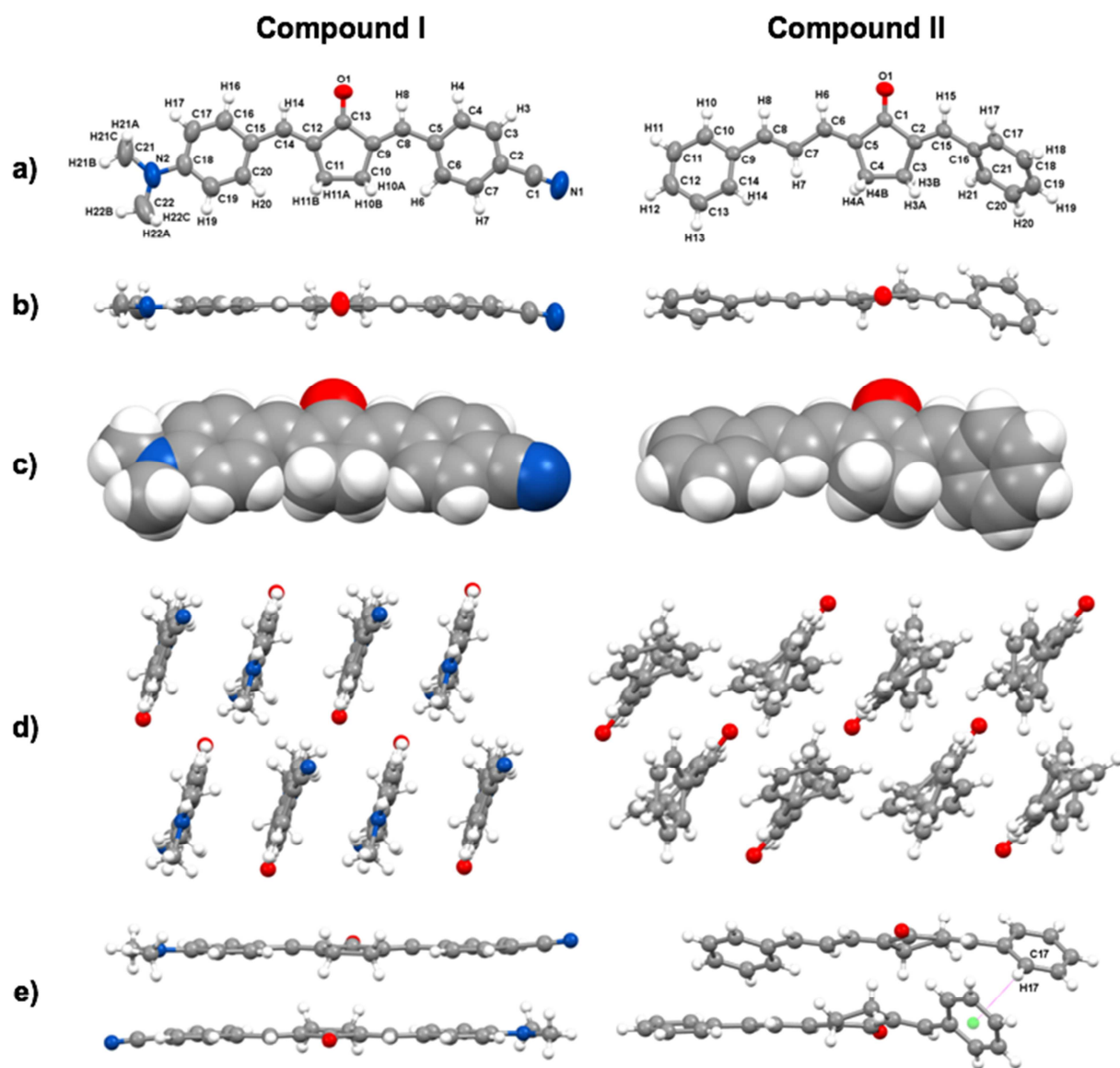
Bond Angles (°)			
	X-ray	DFT	$\Delta$
C <sub>1</sub> -C <sub>2</sub> -C <sub>3</sub>	108.3(1)	109.3	-1.0
C <sub>1</sub> -C <sub>2</sub> -C <sub>15</sub>	121.5(1)	119.2	2.3
C <sub>1</sub> -C <sub>5</sub> -C <sub>4</sub>	108.7(1)	109.8	-1.1
C <sub>1</sub> -C <sub>5</sub> -C <sub>6</sub>	123.5(1)	121.1	2.4
C <sub>2</sub> -C <sub>1</sub> -C <sub>5</sub>	107.6(1)	108.8	-1.2
C <sub>2</sub> -C <sub>1</sub> -O <sub>1</sub>	125.8(1)	126.1	-0.3
C <sub>2</sub> -C <sub>3</sub> -C <sub>4</sub>	104.9(1)	106.0	-1.1
C <sub>2</sub> -C <sub>15</sub> -C <sub>16</sub>	127.7(1)	131.2	-3.5
C <sub>3</sub> -C <sub>2</sub> -C <sub>15</sub>	130.0(1)	131.5	-1.5
C <sub>3</sub> -C <sub>4</sub> -C <sub>5</sub>	105.3(1)	105.7	-0.4
C <sub>4</sub> -C <sub>5</sub> -C <sub>6</sub>	127.8(1)	129.1	-1.3
C <sub>5</sub> -C <sub>1</sub> -O <sub>1</sub>	126.6(1)	126.1	0.5
C <sub>5</sub> -C <sub>6</sub> -C <sub>7</sub>	125.6(1)	126.3	-0.7
C <sub>6</sub> -C <sub>7</sub> -C <sub>8</sub>	123.2(1)	122.6	0.6
C <sub>7</sub> -C <sub>8</sub> -C <sub>9</sub>	127.8(1)	127.9	-0.1
C <sub>8</sub> -C <sub>9</sub> -C <sub>10</sub>	119.3(1)	118.7	0.6
C <sub>8</sub> -C <sub>9</sub> -C <sub>14</sub>	122.8(1)	123.4	-0.6
C <sub>9</sub> -C <sub>10</sub> -C <sub>11</sub>	121.0(1)	121.3	-0.3
C <sub>9</sub> -C <sub>14</sub> -C <sub>13</sub>	120.9(1)	120.9	0.05
C <sub>10</sub> -C <sub>9</sub> -C <sub>14</sub>	117.9(1)	117.9	-0.02
C <sub>10</sub> -C <sub>11</sub> -C <sub>12</sub>	120.2(2)	120.0	0.2
C <sub>11</sub> -C <sub>12</sub> -C <sub>13</sub>	119.8(2)	119.5	0.3
C <sub>12</sub> -C <sub>13</sub> -C <sub>14</sub>	120.3(2)	120.4	-0.1
C <sub>15</sub> -C <sub>16</sub> -C <sub>17</sub>	119.3(1)	117.8	1.5
C <sub>15</sub> -C <sub>16</sub> -C <sub>21</sub>	122.8(1)	124.5	-1.7
C <sub>16</sub> -C <sub>17</sub> -C <sub>18</sub>	120.7(1)	121.4	-0.7
C <sub>16</sub> -C <sub>21</sub> -C <sub>20</sub>	120.9(1)	120.8	0.1
C <sub>17</sub> -C <sub>16</sub> -C <sub>21</sub>	118.0(1)	117.7	0.3
C <sub>17</sub> -C <sub>18</sub> -C <sub>19</sub>	120.3(2)	120.0	0.3
C <sub>18</sub> -C <sub>19</sub> -C <sub>20</sub>	119.7(2)	119.5	0.2
C <sub>19</sub> -C <sub>20</sub> -C <sub>21</sub>	120.3(1)	120.5	-0.2

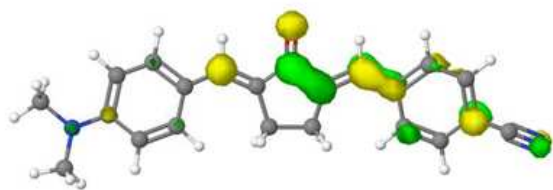
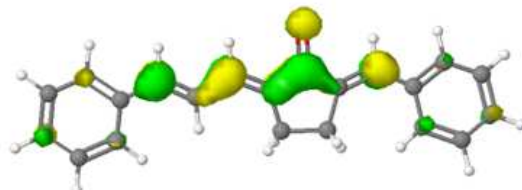
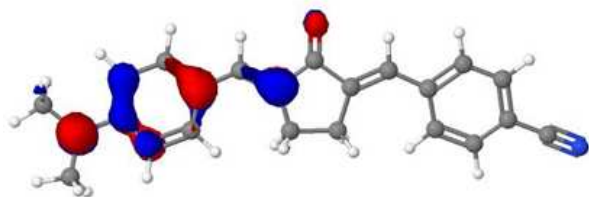
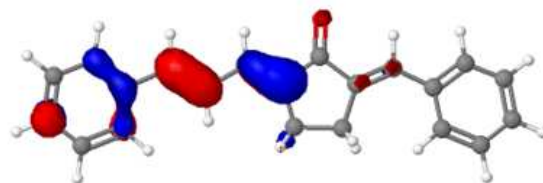
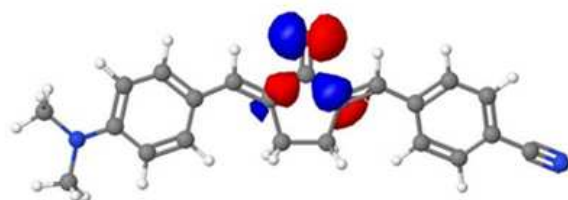
<b>I</b>			
<b>Gas</b>			
State	Energy (cm <sup>-1</sup> )	f	MO Configuration Interaction (CI)
S <sub>1</sub> ( $\pi$ , $\pi^*$ )	21,142 ( $\lambda$ 473 nm)	0.73	HOMO ( $\pi$ ) $\rightarrow$ LUMO ( $\pi^*$ )
S <sub>2</sub> (n, $\pi^*$ )	23,474 ( $\lambda$ 426 nm)	0.00	HOMO - 2 (n) $\rightarrow$ LUMO ( $\pi^*$ )
S <sub>3</sub> ( $\pi$ , $\pi^*$ )	27,248 ( $\lambda$ 367 nm)	0.84	HOMO - 1 ( $\pi$ ) $\rightarrow$ LUMO ( $\pi^*$ ) HOMO ( $\pi$ ) $\rightarrow$ LUMO + 1 ( $\pi^*$ )
<b>Chloroform</b>			
S <sub>1</sub> ( $\pi$ , $\pi^*$ )	19,417 ( $\lambda$ 515 nm)	0.94	HOMO ( $\pi$ ) $\rightarrow$ LUMO ( $\pi^*$ )
S <sub>2</sub> (n, $\pi^*$ )	24,814 ( $\lambda$ 403 nm)	0.00	HOMO - 2 (n) $\rightarrow$ LUMO ( $\pi^*$ )
S <sub>3</sub> ( $\pi$ , $\pi^*$ )	26,596 ( $\lambda$ 376 nm)	0.86	HOMO - 1 ( $\pi$ ) $\rightarrow$ LUMO ( $\pi^*$ ) HOMO ( $\pi$ ) $\rightarrow$ LUMO + 1 ( $\pi^*$ )
<b>II</b>			
<b>Gas</b>			
State	Energy (cm <sup>-1</sup> )	f	MO Configuration Interaction (CI)
S <sub>1</sub> (n, $\pi^*$ )	23,041 ( $\lambda$ 434 nm)	0.00	HOMO - 2 (n) $\rightarrow$ LUMO ( $\pi^*$ )
S <sub>2</sub> ( $\pi$ , $\pi^*$ )	25,316 ( $\lambda$ 395 nm)	1.41	HOMO ( $\pi$ ) $\rightarrow$ LUMO ( $\pi^*$ )
S <sub>3</sub> ( $\pi$ , $\pi^*$ )	28,736 ( $\lambda$ 348 nm)	0.018	HOMO - 1 ( $\pi$ ) $\rightarrow$ LUMO ( $\pi^*$ )
<b>Ethanol</b>			
S <sub>1</sub> ( $\pi$ , $\pi^*$ )	23,810 ( $\lambda$ 420 nm)	1.58	HOMO ( $\pi$ ) $\rightarrow$ LUMO ( $\pi^*$ )
S <sub>2</sub> (n, $\pi^*$ )	24,390 ( $\lambda$ 410 nm)	0.0035	HOMO - 2 (n) $\rightarrow$ LUMO ( $\pi^*$ )
S <sub>3</sub> ( $\pi$ , $\pi^*$ )	28,329 ( $\lambda$ 353 nm)	0.044	HOMO - 1 ( $\pi$ ) $\rightarrow$ LUMO ( $\pi^*$ )

\*The corresponding energies in units of wavelength ( $\lambda$ , nm) are given in parentheses.

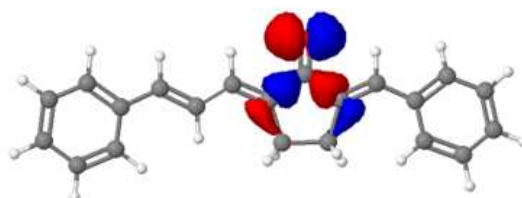






LUMO ( $\pi^*$ )LUMO ( $\pi^*$ )HOMO ( $\pi$ )HOMO ( $\pi$ )

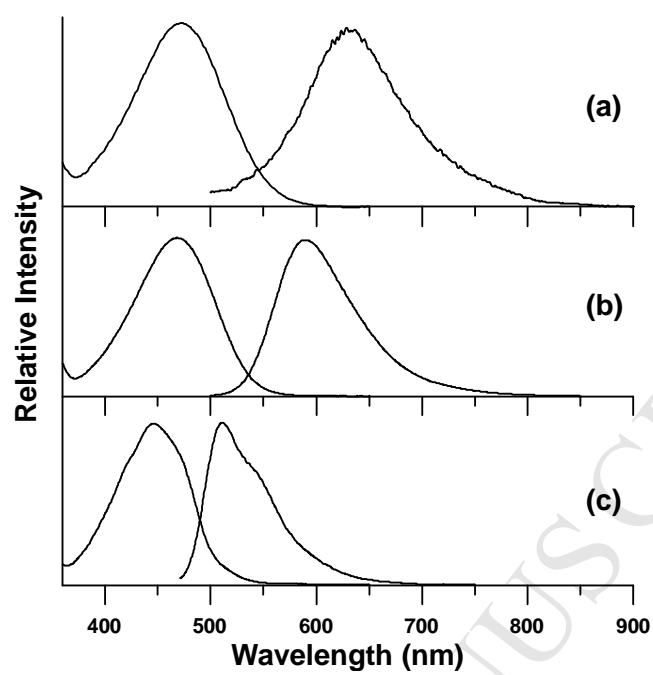
HOMO-2 (n)

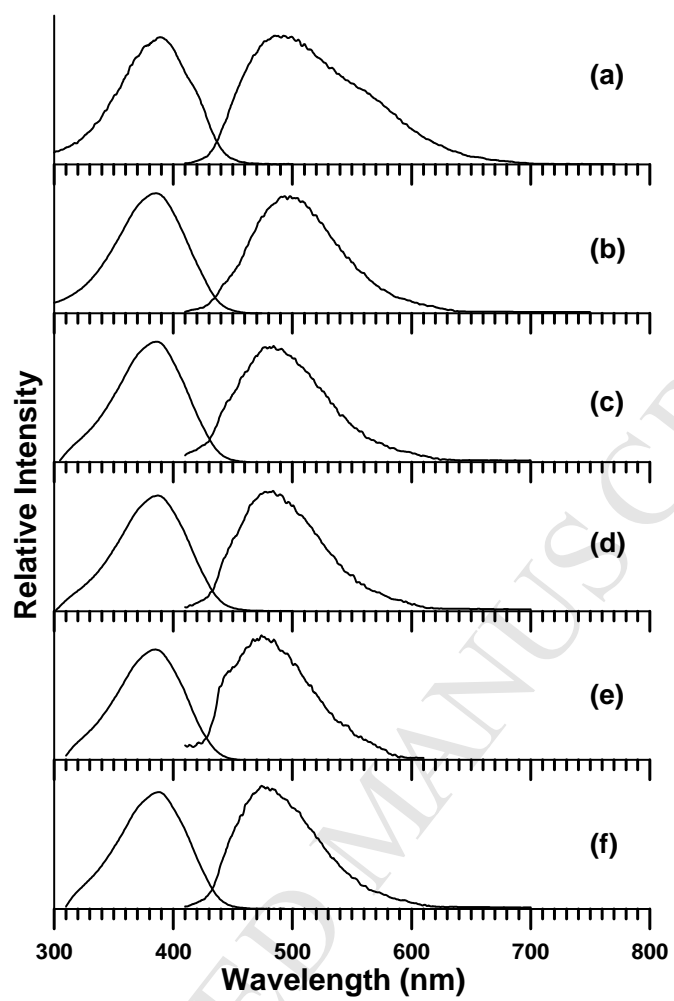
**I**

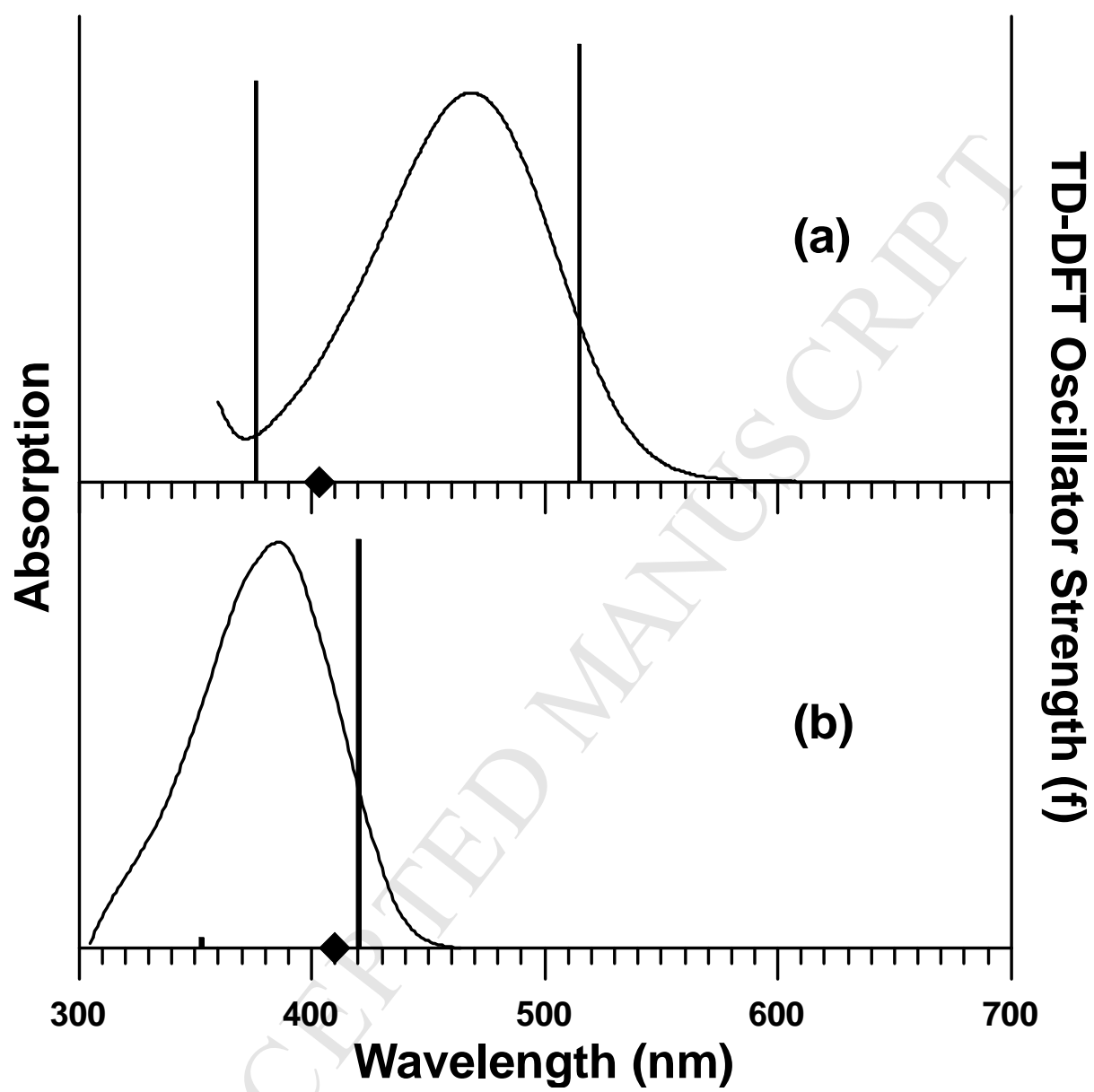
HOMO-2 (n)

**II**

ACCEPTED







### Highlights

- The X-ray crystal structures of (2*E*,5*E*)-2-(4-cyanobenzylidene)-5-(4-dimethylaminobenzylidene)cyclopentanone (**I**) and (2*E*,5*E*)-2-benzylidene-5-cinnamylidenecyclopentanone (**II**) are presented, compared to the gas phase structures calculated using density functional theory.
- Intermediate compounds **IA** and **IIA** were synthesized by the DIMCARB mediated route of an equimole amount of cyclopentanone and corresponding aldehyde. Target compounds **I** and **II** were synthesized by the intermolecular base catalyzed crossed aldol condensation reaction between an equimole amount of either **IA** or **IIA** and the second aldehyde of interest. The % yields of both the intermediate and target compounds were found to range between moderate to high (50 – 100 %).
- The single crystal X-ray structure of **I** was found to be mainly planar and **II** nonplanar. Excellent agreement was established between the experimental single crystal X-ray structure and the predicted DFT structure of **I** and **II** in both bond lengths and bond angles.
- Surveys of the spectroscopic, photophysical, and reactivity properties of these compounds show and explain how molecular structure plays an important role in determining the outcomes of these properties.